AAS 18-350

DYNAMICAL EFFECTS OF SOLAR RADIATION PRESSURE ON THE DEFLECTION OF NEAR-EARTH ASTEROIDS

Luis O. Marchi,[*] D. M. Sanchez,[†] F. C. F. Venditti,[‡] and A. F. B. A. Prado[§]

This work aims to find an alternative solution to the important problem of deflecting asteroids that are coming too close to Earth, with the risk of collision. This alternative is based on the use of a device with a large area/mass ratio attached by a tether to use solar radiation pressure (SRP) to help to deflect the trajectory of the asteroid. The paper describes the dynamics of the system composed by the asteroid, the tether and the device. The model is then used to study the effects that the tether length and the solar radiation pressure (acting on the surface of the device) exert on the deflection of a larger Potentially Hazardous Asteroid (PHA). As a starting point, the tether is assumed to be inextensible and massless and the motion is described only in the plane of the orbit of the PHA around the Sun.

INTRODUCTION

Although found practically everywhere throughout the Solar System, most asteroids and comets are concentrated in three major locations: the Asteroid Belt, the Kuiper Belt, and the Oort Cloud. Particularly, Potentially Hazardous Asteroids (PHAs) have become the research object for several scientists around the world, due to the real possibilities of an impact with Earth. There are strong evidences that, in the past, the extinction of dinosaurs was triggered by the impact of an asteroid on the Yucatan Peninsula, in Mexico. At least two records of smaller magnitudes can also be found in Russia: Tunguska in 1908, and Chelyabinsk in 2013. In the literature, there are many studies dedicated to the characterization of these rocky bodies, such as shape, size, spin state, and composition, which are necessary for space missions[1,2,3]. This information is also important to understand the origin of planetary systems, since small bodies are remnants from the formation of the Solar System.

During the last decades, one can note the scientific effort to develop asteroid deflection techniques. The strategies can be classified depending on the characteristics of the asteroid and the time available to fulfill the mission. The change in angular momentum of an asteroid can be performed through the use of kinetic impactors, nuclear interceptors and mass drivers[4]. In 2022, for example, NASA's DART mission plans to measure the effects of the first kinetic impact experiment, whose target will be the binary near-Earth asteroid system Didymos[5]. Low-thrust possibilities can also be considered, such as gravity tractors; or passive, such as changes on the surface of the asteroid by

[*] National Institute for Space Research, Space Mechanics and Control, Doctoral Student, Astronautas Avenue 1758, São José dos Campos-SP, Brazil, 12227-010.
[†] National Institute for Space Research, Space Mechanics and Control, Postdoctoral Researcher, Astronautas Avenue 1758, São José dos Campos-SP, Brazil, 12227-010.
[‡] Arecibo Observatory, Planetary Radar, Arecibo-PR, USA, 00612.
[§] National Institute for Space Research, Space Mechanics and Control, General Coordinator of the Graduate School, Astronautas Avenue 1758, São José dos Campos-SP, Brazil, 12227-010.

thermal induction[6,7], which one example was a study using a tethered system formed by an asteroid and a solar sail[8]. The gravity tractor is a technique that uses the perturbation of the mass of a spacecraft that is positioned near the asteroid[9], also there are studies of formation flying with solar sails and gravity tractor combined to optimize the deflection[10]. It is a weak force, so it is necessary longer times to deflect the trajectory of the asteroid. In this technique, times of the order of hundreds of years need to be considered. Another technique is the displacement of the center of mass of the PHA that can be achieved by attaching a long tether and a ballast mass[11,12,13], or even a small asteroid[14,15,16].

In this work, a deflection method consisting of a device connected to the PHA with a tether is proposed. Space tethers are long cables with several different proposed applications, such as: space elevators[17,18], tether satellite systems[19], debris removal[20], electrodynamic tethers for power[21], but not limited to these applications. The main objective is to analyze the influence of the solar radiation pressure on the dynamics of the PHA-tether-device system. Solar radiation pressure can affect the position of small particles in space[22]. The Yarkovsky and YORP effects, which are SRP driven phenomenon, can also alter the trajectory of small asteroids, according to its physical properties[23,24]. The smaller the body, the higher will be perturbation generated on its orbit. Solar radiation pressure can also affect asteroids indirectly, for example, by placing a solar sail on it in order to change its trajectory, and even for asteroid de-spin to optimize the deflection[25,26]. It is expected that these effects become more evident in regions of closer approximations to the Sun. The perturbation effects on the PHA trajectory is quantified as the minimum distance of the asteroid with respect to the Earth, before and after the tether and the device are attached to the PHA. It is also measured the differences between the perturbed and unperturbed orbits of the PHA.

The major advantage of using the tether-device technique is that it is not necessary to fragment the PHA to change its orbit, as proposed in the impact method, or to move larger masses to the neighborhood of the PHA. There is also no fuel consumption involved after the system is built, which is another advantage of the technique suggested here. Another application of this strategy would be to transfer these bodies closer to Earth to explore them scientifically or commercially. An example is the ongoing Osiris-Rex mission, which the goal is to return a sample of the asteroid Bennu in 2023[27,28]. A technique to approximate asteroids to the Earth will help future missions of this type, as well as asteroid mining missions.

MATHEMATICAL MODEL

In this section, we will explain the development of the mathematical model composed by an asteroid fixed by a tether to a device with a reflective surface. The physical model is two-dimensional and the whole dynamics of the problem is described in the plane of the orbit of the asteroid around the Sun. Due to this first simplifying hypothesis, asteroids that have low inclinations with respect to the plane of the ecliptic are chosen for the numerical simulations.

The system can be seen in Figure 1. In this figure we have two main reference systems. The inertial system (*XY*), originating in the Sun, and that is represented by the unit vectors $\{\hat{e}_1, \hat{e}_2\}$. The unit vectors $\{\hat{a}_1, \hat{a}_2\}$ refer to the rotational system (*xy*), with origin in the center of mass of the asteroid. The letters *S*, *A*, *B* and *P* refer to the Sun, center of mass of the PHA, the point of attachment of the device and the point of attachment of the tether, respectively. There is a large number of variables that appear in this system: m_A is the mass of the PHA, A_B/m_B is the area-to-mass ratio of the device, *M* is the mass of the Sun, *R* is the distance between the Sun and PHA, r_{PA} is the distance between the center of mass and the point of attachment of the PHA, r_B is the distance between the PHA and the device, R_B is the distance between the Sun and the device, l is the length of the tether, ν is the true anomaly of the PHA, θ is the rotation angle of the PHA, α is the angle that the tether makes with the PHA, ψ is the angle between the perihelion of the Earth and the perihelion of the PHA, η is the angle between R_{SA} and R_{SB}, ξ is the angle between R_{PA} and the x-axis of the reference system (xy), φ is the angle between R_{PA} and R_{AB}, F_{GR} is the gravitational force of attraction, and F_{PR} is the force due to the solar radiation pressure.

In this first study it is assumed that the tether is rigid and massless. The angle α is assumed to be constant, which means that the tether is fixed in the PHA such that it is not possible to rotate the device with respect to the PHA. This is done to allow shorter tethers without having the problem of the device rolling around the PHA.

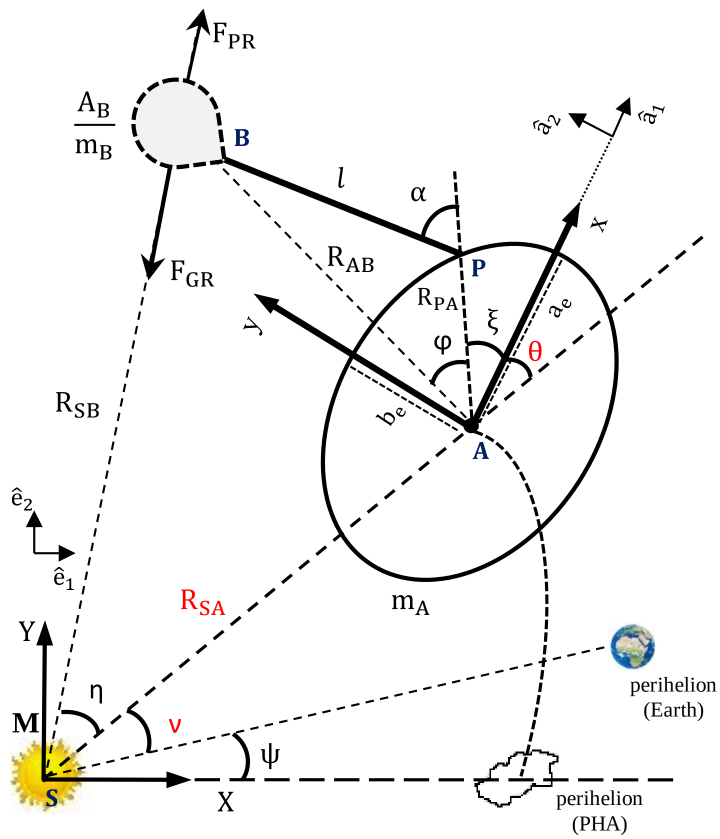

Figure 1. Two-dimensional physical model of the Sun-PHA-Device system.

The goal is to use a device to increase the effect of SRP on the system, consequently changing the initial trajectory of the PHA. The angle α is assumed to be constant (the tether has no pendular motion) in order to keep the position of m_B fixed with respect to m_A. This hypothesis facilitates the modeling phase, because the position of the center of mass of the system does not change with time. In addition, only m_A has rotation about its own axis. In the model adopted here we have three degrees of freedom (or generalized coordinates), which are: R_{SA}, ν and θ.

Figure (2) illustrates the geometry required to determine the velocities of the PHA and the device relative to the inertial (XY) system. Two intermediate reference systems called ($x'y'$) and ($x''y''$) are used in the transformation of coordinates of the device from the body system (xy) to the inertial system (XY).

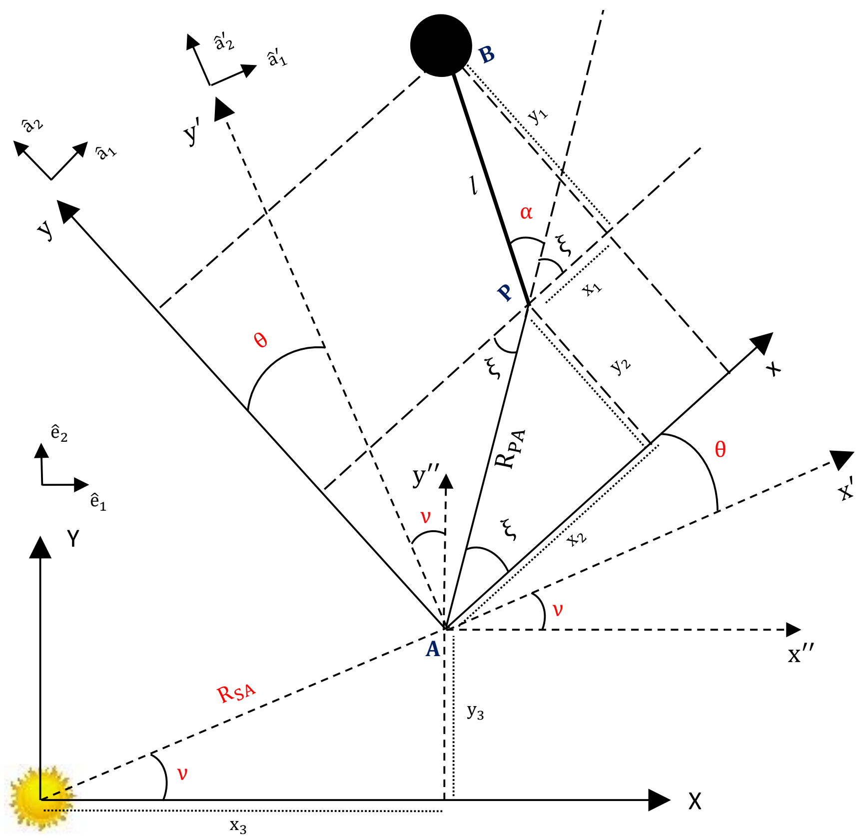

Figure 2. Geometry used to determine the velocities of the PHA and the device in the inertial coordinate system.

The position and velocity vectors of the center of mass of the PHA and the device, in this order, described in the inertial coordinate system, are given by equations (1) to (4):

$$\vec{r}_{A_{XY}} = R_{SA}\cos(\nu)\hat{e}_1 + R_{SA}\sin(\nu)\hat{e}_2 \tag{1}$$

$$\vec{v}_{A_{XY}} = \left[\dot{R}_{SA}\cos(\nu) - R_{SA}\dot{\nu}\sin(\nu)\right]\hat{e}_1 + \left[\dot{R}_{SA}\sin(\nu) + R_{SA}\dot{\nu}\cos(\nu)\right]\hat{e}_2 \tag{2}$$

$$\begin{aligned}\vec{r}_{B_{XY}} = {} & [l\cos(\alpha + \xi + \theta + \nu) + R_{PA}\cos(\xi + \theta + \nu) + R_{SA}\cos(\nu)]\hat{e}_1 \\ & + \ [l\sin(\alpha + \xi + \theta + \nu) + R_{PA}\sin(\xi + \theta + \nu) + R_{SA}\sin(\nu)]\hat{e}_2\end{aligned} \tag{3}$$

$$\begin{aligned}\vec{v}_{B_{XY}} = {} & \left[\dot{R}_{SA}\cos(\nu) - R_{SA}\dot{\nu}\sin(\nu) - R_{PA}\sin(\xi + \theta + \nu)\left(\dot{\theta} + \dot{\nu}\right) - l\sin(\alpha + \xi + \theta + \nu)\left(\dot{\theta} + \dot{\nu}\right)\right]\hat{e}_1 \\ & + \left[\dot{R}_{SA}\sin(\nu) + R_{SA}\dot{\nu}\cos(\nu) + R_{PA}\cos(\xi + \theta + \nu)\left(\dot{\theta} + \dot{\nu}\right) \right. \\ & \left. + \, l\cos(\alpha + \xi + \theta + \nu)\left(\dot{\theta} + \dot{\nu}\right)\right]\hat{e}_2\end{aligned} \tag{4}$$

From equations (2) and (4), we have the following scalar products:

$$\vec{v}_{A_{XY}} . \vec{v}_{A_{XY}} = \dot{R}_{SA}^2 + R_{SA}^2\dot{\nu}^2 \tag{5}$$

$$\begin{aligned}\vec{v}_{B_{XY}} . \vec{v}_{B_{XY}} = {} & \dot{R}_{SA}^2 + R_{SA}^2\dot{\nu}^2 + l^2\left(\dot{\theta} + \dot{\nu}\right)^2 + R_{PA}^2\left(\dot{\theta} + \dot{\nu}\right)^2 \\ & + 2\left(\dot{\theta} + \dot{\nu}\right)\left[lR_{PA}\left(\dot{\theta} + \dot{\nu}\right)\cos(\alpha) + R_{PA}R_{SA}\dot{\nu}\cos(\xi + \theta) + lR_{SA}\dot{\nu}\cos(\alpha + \xi + \theta) \right. \\ & \left. - \dot{R}_{SA}R_{PA}\sin(\xi + \theta) - l\dot{R}_{SA}\sin(\alpha + \xi + \theta)\right]\end{aligned} \tag{6}$$

The total translational kinetic energy is composed by two parts, the first one associated to the PHA and the second one to the device, according to Equation (7).

$$T_{TK} = \frac{1}{2} m_A \left(\vec{v}_{A_{XY}} . \vec{v}_{A_{XY}}\right) + \frac{1}{2} m_B \left(\vec{v}_{B_{XY}} . \vec{v}_{B_{XY}}\right) \tag{7}$$

It was assumed that only the PHA has rotation about its own axis. In Equation (8) we have that the total rotational kinetic energy is given by:

$$T_{TR} = \frac{1}{2} I_A \left(\dot{\theta} + \dot{\nu}\right)^2 \tag{8}$$

where I_A refers to the moment of inertia.

Three formulations are used to calculate the moment of inertia at the center of mass of the PHA. The first and second were used when only the PHA is considered, while the third one is an approximation for the PHA-Tether-Device system.

$$I_A = \begin{cases} \frac{2}{5} m_A R_0^2, & \text{(PHA: spherical equator)} \\ \frac{1}{5} m_A (a_e^2 + b_e^2), & \text{(PHA: ellipsoidal equator)} \\ \frac{m_A m_B}{m_A + m_B} R_{AB}^2 + (m_A + m_B)\left(\frac{m_B R_{AB}}{m_A + m_B}\right)^2, & \text{(PHA} - \text{Tether} - \text{Device)} \end{cases} \tag{9}$$

where R_0 is the characteristic length of the asteroid and a_e and b_e are the dimensions of the ellipse.

Therefore, by replacing equations (5) and (6) in equation (7) and summing the expression obtained with equation (8), we have that the total kinetic energy of the system is given by:

$$\begin{aligned} T_{TOT} = {} & \frac{1}{2}(m_A + m_B)\left[\dot{R}_{SA}^2 + R_{SA}^2 \dot{\nu}^2\right] + \frac{1}{2}\left(\dot{\theta} + \dot{\nu}\right)^2 \left[m_B\left(l^2 + R_{PA}^2\right) + I_A\right] \\ & + m_B\left(\dot{\theta} + \dot{\nu}\right)\left[l R_{PA}\left(\dot{\theta} + \dot{\nu}\right)\cos(\alpha) + R_{PA} R_{SA} \dot{\nu} \cos(\xi + \theta) + l R_{SA} \dot{\nu} \cos(\alpha + \xi + \theta) \right. \\ & \left. - \dot{R}_{SA} R_{PA} \sin(\xi + \theta) - l \dot{R}_{SA} \sin(\alpha + \xi + \theta)\right] \end{aligned} \tag{10}$$

The acceleration due to the solar radiation pressure can be expressed as [29]:

$$\ddot{\vec{P}}_R = -C_r P_{rad} \frac{A_B}{m} \left(\frac{D_M}{|\vec{r}_A - \vec{r}_S|}\right)^2 \frac{\vec{r}_A - \vec{r}_S}{|\vec{r}_A - \vec{r}_S|} \tag{11}$$

where C_r is the solar radiation pressure coefficient (1 for maximum absorption and 2 for maximum reflexivity), P_{rad} is the solar radiation pressure with respect to the celestial body, A_B is the area exposed to the Sun, *m* is the mass of the body, D_M is refered to the average distance of the body, $\vec{r}_A$ is the position vector of the asteroid and $\vec{r}_S$ is the position vector of the Sun.

In the case under study, the gravity and the solar radiation pressure are conservative forces, because they depend only on the position of the device relative to the Sun. The phenomena of occultation made by the PHA in the device is not considered. Also, the SRP on the PHA is neglected, and only the effects of the SRP on the device is analyzed. A more detailed study would need to take this effect into account, but it is not in the scope of the present paper. The absolute value of the solar radiation pressure force, written mathematically from the variables used in the problem addressed in this work, can be expressed as:

$$\mathrm{F_R} = \mathrm{C_r P_{rad} A_B} \left(\frac{\mathrm{D_M}}{\mathrm{R_{SB}}}\right)^2 \tag{12}$$

where A_B is the cross-sectional area of the device and R_{SB} is the distance between the Sun and the device.

To simplify the problem, it is assumed that D_M is equivalent to the average distance between the Earth and the Sun (AU = 149,597,870,700 m) and that $P_{rad} = 4.56 \text{ x } 10^{-6}$ N/m² (at the Sun-Earth system). We also have $GM = 1.32754 \text{ x } 10^{20}$ m³/s². The dimensionless parameter β is defined as the ratio between the force of radiation pressure and the force of the gravity acting on the device.

$$\beta = \frac{\mathrm{F_{PR}}}{\mathrm{F_{GR}}} = \frac{\frac{\mathrm{C_r P_{rad} A_B} D_M{}^2}{\mathrm{R_{SB}^2}}}{\frac{\mathrm{GMm_B}}{\mathrm{R_{SB}^2}}} = \mathrm{C_r P_{rad}} \frac{D_M{}^2}{\mathrm{GM}} \frac{\mathrm{A_B}}{\mathrm{m_B}} \tag{13}$$

Therefore, the equation that relates A_B/m_B as a function of the β parameter is:

$$\frac{\mathrm{A_B}}{\mathrm{m_B}} = \begin{cases} 8.67244 \text{ x } 10^2\ \beta, & for \quad \mathrm{C_r} = 1.5 \\ 6.67110 \text{ x } 10^2\ \beta, & for \quad \mathrm{C_r} = 1.95 \end{cases} \tag{14}$$

The force due to the solar radiation pressure always acts contrary to the gravitational force. Thus, the resulting force acting on the device, written as a function of the parameter β, is:

$$\mathrm{F_{RES}} = \mathrm{F_{GR}} - \mathrm{F_{PR}} = (1 - \beta) \frac{\mathrm{GMm_B}}{\mathrm{R_{SB}}^2} \tag{15}$$

From Equation (15) and the definition of potential, we have that the potential between the Sun and the device is given by:

$$\mathrm{V_{SB}} = \frac{1}{\mathrm{m_B}} \int_{\infty}^{\mathrm{R_{SB}}} \frac{\mathrm{GMm_B}}{\mathrm{R_{SB}}^2} (1 - \beta)\, \mathrm{dR_{SB}} = -\frac{\mathrm{GM}}{\mathrm{R_{SB}}} (1 - \beta) \tag{16}$$

The position of the device relative to the PHA is kept fixed. This implies that there is no gravitational potential between these bodies. Therefore, the total gravitational potential of the system is:

$$\mathrm{V_{TOT}} = -\frac{\mathrm{GM}}{\mathrm{R_{SA}}} - \mathrm{GM}(1 - \beta) \left[\frac{1}{\mathrm{R_{SA}}} - \frac{\mathrm{R_{AB}}}{\mathrm{R_{SA}^2}} \cos(\theta + \xi + \varphi)\right] \tag{17}$$

The gravitational potential energy is defined as the potential per unit mass. Therefore, its total value for the system being studied is:

$$U_{TOT} = -\frac{GM}{R_{SA}}[m_A + m_B(1-\beta)] + m_B(1-\beta)GM\frac{R_{AB}}{R_{SA}^2}\cos(\theta+\xi+\varphi) \tag{18}$$

The Lagrangian of the system is given by the subtraction between the kinetic and potential energies.

$$\begin{aligned}\mathcal{L} = T_{TOT} - U_{TOT} \\ &= \frac{1}{2}(m_A + m_B)\left[\dot{R}_{SA}^2 + R_{SA}^2\dot{\nu}^2\right] \\ &+ \frac{1}{2}\left(\dot{\theta}+\dot{\nu}\right)^2\left[m_B\left(l^2 + R_{PA}^2\right) + I_A\right] + m_B\left(\dot{\theta}+\dot{\nu}\right)\left[lR_{PA}\left(\dot{\theta}+\dot{\nu}\right)\cos(\alpha) \right. \\ &+ R_{PA}R_{SA}\dot{\nu}\cos(\xi+\theta) + lR_{SA}\dot{\nu}\cos(\alpha+\xi+\theta) - \dot{R}_{SA}R_{PA}\sin(\xi+\theta) \\ &\left. - l\dot{R}_{SA}\sin(\alpha+\xi+\theta)\right] + m_A\frac{GM}{R_{SA}} \\ &+ m_B(1-\beta)\left[\frac{GM}{R_{SA}} - GM\frac{R_{AB}}{R_{SA}^2}\cos(\theta+\xi+\varphi)\right]\end{aligned} \tag{19}$$

The system's equations of motion are obtained from the Lagrange equation assuming that the generalized forces are zero.

$$\frac{d}{dt}\left(\frac{\partial\mathcal{L}}{\partial\dot{q}_i}\right) - \frac{\partial\mathcal{L}}{\partial q_i} = 0 \tag{20}$$

where $q_i \equiv R_{SA}, \nu, \theta$ are the generalized coordinates (degrees of freedom of the system).

The second-order differential equations describing the motion of the PHA-Tether-Device system are:

For R_{SA}:

$$\begin{aligned}(m_A + m_B)\left[\ddot{R}_{SA} - R_{SA}\dot{\nu}^2\right] + \frac{GM}{R_{SA}^2}\left[m_A + m_B(1-\beta)\left(1 - 2\frac{R_{AB}}{R_{SA}}\cos(\theta+\xi+\varphi)\right)\right] \\ - m_B\dot{\theta}\left(\dot{\nu}+\dot{\theta}\right)[R_{PA}\cos(\theta+\xi) + l\cos(\alpha+\xi+\theta)] \\ - m_B\dot{\nu}\left(\dot{\nu}+\dot{\theta}\right)[R_{PA}\cos(\theta+\xi) + l\cos(\alpha+\xi+\theta)] \\ - m_B\left(\ddot{\nu}+\ddot{\theta}\right)[R_{PA}\sin(\theta+\xi) + l\sin(\alpha+\xi+\theta)] = 0\end{aligned} \tag{21}$$

For ν :

$$\begin{aligned}\ddot{\nu}\left[m_B\left(2lR_{PA}\cos(\alpha) + l^2 + R_{PA}^2\right) + 2m_BR_{SA}\left(l\cos(\alpha+\xi+\theta) + R_{PA}\cos(\xi+\theta)\right) \right. \\ \left. + (m_A + m_B)R_{SA}^2\right] \\ + m_B\left[\ddot{\theta}\left(lR_{SA}\cos(\alpha+\xi+\theta) + 2lR_{PA}\cos(\alpha) + l^2 + R_{PA}^2 \right.\right. \\ \left. + R_{PA}R_{SA}\cos(\xi+\theta)\right) - \ddot{R}_{SA}\left(l\sin(\alpha+\xi+\theta) + R_{PA}\sin(\xi+\theta)\right) \\ \left. - \dot{R}_{SA}\dot{\theta}\left(l\cos(\alpha+\xi+\theta) + R_{PA}\cos(\xi+\theta)\right)\right] \\ + 2\dot{\nu}\left[\dot{R}_{SA}\left(m_B\left(l\cos(\alpha+\xi+\theta) + R_{PA}\cos(\xi+\theta)\right) + (m_A + m_B)R_{SA}\right) \right. \\ \left. - m_BR_{SA}\dot{\theta}\left(l\sin(\alpha+\xi+\theta) + R_{PA}\sin(\xi+\theta)\right)\right] \\ + m_B\dot{\theta}\left[\dot{R}_{SA}\left(l\cos(\alpha+\xi+\theta) + R_{PA}\cos(\xi+\theta)\right) \right. \\ \left. - R_{SA}\dot{\theta}\left(l\sin(\alpha+\xi+\theta) + R_{PA}\sin(\xi+\theta)\right)\right] + I_A\left(\ddot{\theta}+\ddot{\nu}\right) \\ = 0\end{aligned} \tag{22}$$

For θ :

$$
\begin{aligned}
-m_B\ddot{R}_{SA}\big(R_{PA}\sin(\xi+\theta)+l\sin(\alpha+\xi+\theta)\big)& \\
+\, m_B\dot{\nu}\big[\dot{R}_{SA}\big(R_{PA}\cos(\xi+\theta)+l\cos(\alpha+\xi+\theta)\big)& \\
-\, R_{SA}\dot{\theta}\big(R_{PA}\sin(\xi+\theta)+l\sin(\alpha+\xi+\theta)\big)\big]+I_A\big(\ddot{\theta}+\ddot{\nu}\big)& \\
+\, m_B\Big[-\dot{R}_{SA}\dot{\theta}\big(R_{PA}\cos(\xi+\theta)+l\cos(\alpha+\xi+\theta)\big)& \\
+\,\ddot{\theta}\left(l^2+R_{PA}^2+2lR_{PA}\cos(\alpha)\right)& \\
+\,\ddot{\nu}\left(l^2+R_{PA}^2+2lR_{PA}\cos(\alpha)+R_{PA}R_{SA}\cos(\xi+\theta)+lR_{SA}\cos(\alpha+\xi+\theta)\right)\Big]& \\
-\, m_B\big(\dot{\nu}+\dot{\theta}\big)\big[-\dot{R}_{SA}R_{PA}\cos(\xi+\theta)-l\dot{R}_{SA}\cos(\alpha+\xi+\theta)-R_{SA}R_{PA}\dot{\nu}\sin(\xi+\theta)& \\
-\, lR_{SA}\dot{\nu}\sin(\alpha+\xi+\theta)\big]-\frac{GMm_B(1-\beta)R_{AB}\sin(\varphi+\xi+\theta)}{R_{SA}^2}=0 \qquad (23)&
\end{aligned}
$$

In Figure 3 the two main parameters are shown, which are calculated to quantify the deviations, and thus, the efficiency of the proposed method. Both are calculated by using the distance between two points in the Cartesian plane.

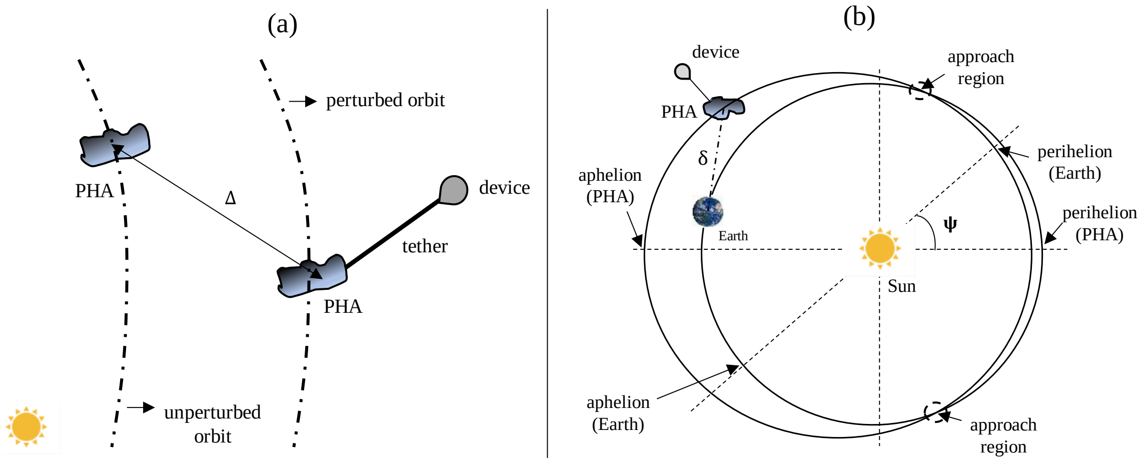

Figure 3. Parameters of deviation between (a) perturbed and unperturbed trajectory (b) PHA-Tether-Device system and Earth. (Adapted from reference 11).

Table 1 shows some parameters of the PHAs chosen for the study, where m_A, a, e and I are the mass, semi-major axis, eccentricity and inclination, respectively. The orbital period around the Sun and the period of rotation are also listed below.

Table 1. Parameters of asteroids used in the numerical simulations.

Object	Mass (kg)	*a* (km)	*e*	*I* (deg)	Orbital Period (days)	Rotation Period (h)
Apophis	2.699×10^{10}	1.37995×10^{8}	0.1912	3.331	323.597	30.4
Itokawa	3.5×10^{10}	1.98087×10^{8}	0.2802	1.621	556.537	12.132
Apollo	3.35×10^{12}	2.19933×10^{8}	0.5598	6.353	651.098	3.065

RESULTS AND ANALYSIS

In this section we will show and discuss the results obtained from the numerical simulations. The simulation time for all the cases is 600 terrestrial years. The two main parameters for quantifying the deviations (Δ and δ) were defined in the previous section. The scientific community estimates that, in the coming decades, it will be possible to design materials with densities of 1 g/m² and even 0.1 g/m², to be used in solar sails in long-term interstellar missions[30,31,32]. Assuming that the solar sail is a spherical device used in the technique proposed in the present paper, we have $A_B/m_B = 1/4\rho$. The dimensions of the device were obtained according to their masses (assumed to be 2,000 kg and 20,000 kg). In addition, the values corresponding to the dimensionless variable β were obtained for the coefficients of reflectivity (C_r) of 1.5 and 1.95. Table 2 contains the values of all the parameters mentioned before. Note that the radius of the spherical device are 3989.423 m and 1261.566 m.

Table 2. Physical Device Parameters.

Density	A_B/m_B	$m_B = 2,000$ kg	$m_B = 20,000$ kg	$C_r = 1.5$	$C_r = 1.95$
[g/m²]	[m²/kg]	Radius [m]	Radius [m]	β	β
0.1	2500	1261.566	3989.423	2.8827	3.7475
1	250	398.942	1261.566	0.2882	0.3747

To facilitate the analysis, $\alpha = 10\,°$ and $\xi = 30\,°$ were considered in all simulations, as examples. The device was inserted into the simulation after 1.2 orbital periods of the PHA. The influence of the variations of these three parameters in the results will be the object of future studies. At the beginning of the simulation the bodies were positioned in the periapsis of their orbits. It was also assumed that there is no lag between the apsidal lines of the Earth and the PHA ($\psi = 0°$). This orbital configuration made it possible to demonstrate two types of missions where the technique suggested in this work can be applicable. In planetary defense it is necessary to deflect the orbit of the PHA to send it away from the Earth, while in space mining it is desirable to approximate the orbit of the PHA to the orbit of the Earth. The results that will be discussed next show that the use of the device could prevent the collision of Itokawa with the Earth in 579 years. In addition, it is possible to reduce the distance of the orbit of Apophis with respect to the orbit of the Earth in 574.5 years, making it possible to send a spacecraft for mining purposes. Of course those time frames are long, but much faster results can be obtained using more than one device to collect the solar radiation pressure.

In Figure 4, we have the variation of Δ/R_E for the 2,000 kg device fixed by tethers to asteroid Itokawa with lengths of 50 km, 500 km and 5,000 km. When the SRP is zero (green curve), the longer the tether, the larger the deviations, but the values are really small, in the order of 0.0045 R_E after 600 years for the 50 km tether, 0.045 R_E after 600 years for the 500 km tether and 0.45 R_E after 600 years for the 5,000 km tether. There is almost a linear relation between the deviations and the length of the tether. In this case, the physical principle that causes the deviation is related to the displacement of the center of mass of the system. Those deviations are small, because the mass of the device is 1.75×10^7 times smaller than the mass of Itokawa, which makes the change in the center of the mass of the system. By including the SRP effect (blue and red curves), the first fact observed is that the higher the coefficient of reflectivity, the larger the deviations. The amplitude of oscillations of the red line is greater compared to the blue one. The maximum deviations are about 1 R_E

higher. It is also noted short period oscillations with an increasing magnitude with time. This increase in the amplitude of oscillations is almost linear in all simulations, with values of the order of deviations of 1 R_E every 150 years for the red line and 0.85 R_E per 150 years for the blue line. The increase in the length of the tether decreases by small amounts the variation in the magnitude of Δ/R_E, because the effects coming from the solar radiation pressure dominates the effects of the variation of the center of the mass of the system.

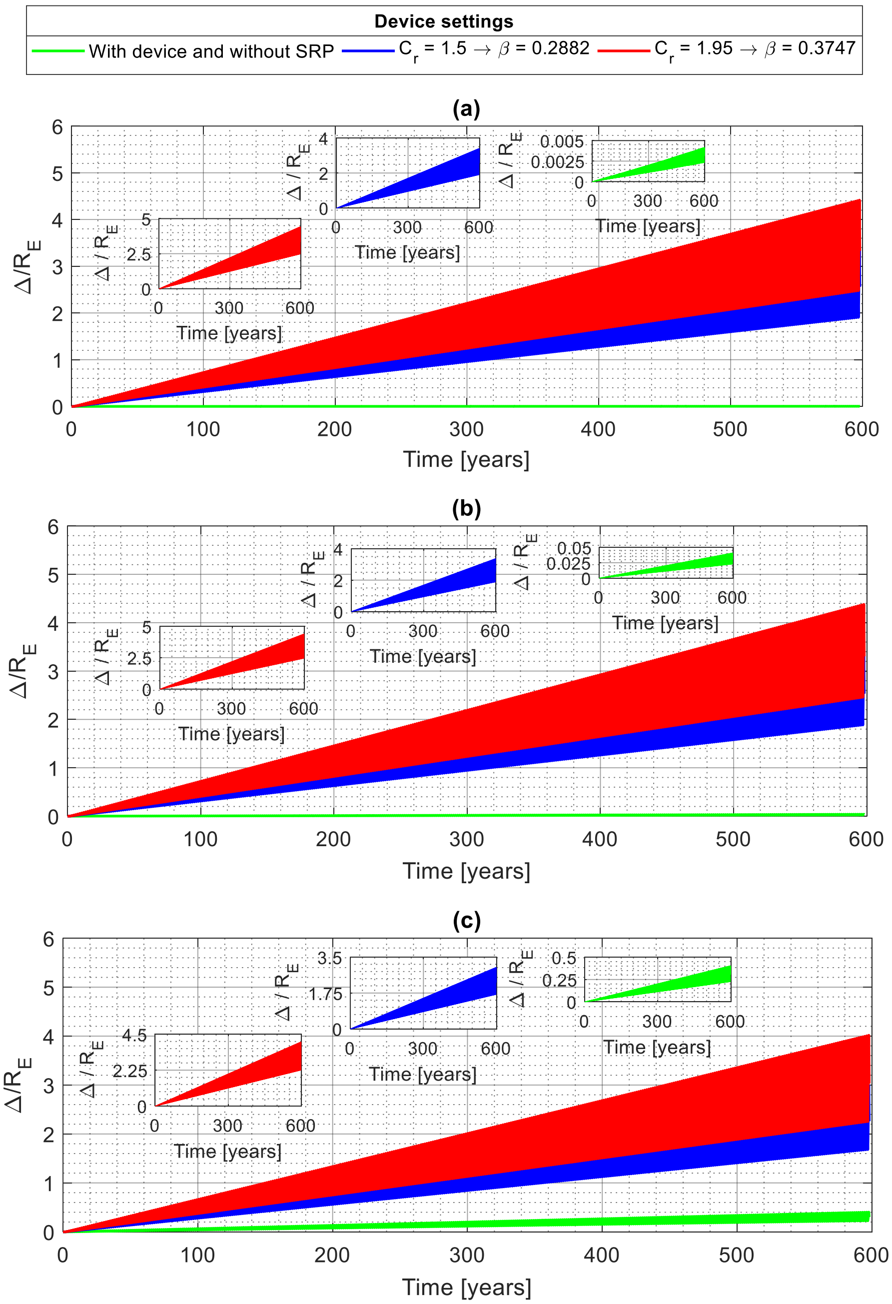

Figure 4. Deviation between the undisturbed and the disturbed orbit in terrestrial radius for Itokawa considering ρ = 1 g/m², a 2,000 kg device and tether lengths of (a) 50 km (b) 500 km (c) 5,000 km.

In Figure 5, we have the variation Δ/R_E for a tether with 50 km and a device with mass of 20,000 kg. Compared to the previous results, it is noticed that the deviations increased approximately by a factor of 10, which shows its almost linear relation with the mass of the device.

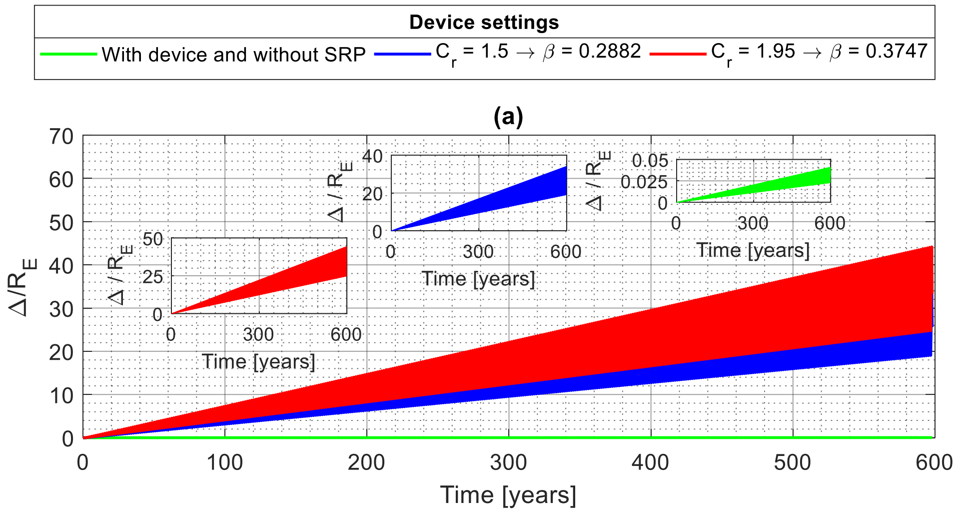

Figure 5. Deviation between the undisturbed and the disturbed orbit in terrestrial radius for Itokawa considering ρ = 1 g/m², a 20,000 kg device and tether length of 50 km.

Table 3 shows that the differences in Δ due to the increased tether length are small (of the order of 10%) and do not depend on the reflectivity coefficient (C_r). These differences are, in fact, proportional to the increase in the tether length, and also, of the mass of the device (by a factor of 10). It was also verified that the tether length slightly changes the deviation with respect to Earth (δ) when the SRP is being considered. In structural terms, shorter length tethers are easier to construct. Therefore, the results that will be presented below are for tethers of 50 km.

Table 3. Effect of the tether length at t = 600 years considering a device with ρ = 1 g/m² connected to Itokawa.

Device mass [kg]	**$\vert\Delta_{50km} - \Delta_{500km}\vert$ $[R_E]$**		**$\vert\Delta_{50km} - \Delta_{5000km}\vert$ $[R_E]$**	
	$C_r = 1.5$	**$C_r = 1.95$**	**$C_r = 1.5$**	**$C_r = 1.95$**
2,000	0.04	0.04	0.4	0.4
20,000	0.4	0.4	4	4

In Figure 6, the results of the Δ/R_E variations for the asteroid Apophis are shown. Its mass is approximately 22.9% lower than the mass of Itokawa. This fact explains why Δ/R_E has larger variations in magnitude when compared to Itokawa. The rate of the increase of the deviations with time is about 1 R_E per 100 years when using a device with 2,000 kg and 1 R_E per 10 years when using a device with 20,000 kg and C_r = 1.95. To verify the relation that the deflection technique suggested in this work has with the asteroid mass, an additional study was carried out using asteroid Apollo, which has a mass of 3.35×10^{12} kg. Although it has a more eccentric orbit compared to Apophis and Itokawa, since it is more massive, the variation of Δ/R_E, in 600 years, is approximately

0.52 for a 2,000 kg device and Cr = 1.95. Therefore, we can preliminarily conclude that, for the parameters considered for the device, the technique would be effective for asteroids with mass of the order of 10^{10} kg or less.

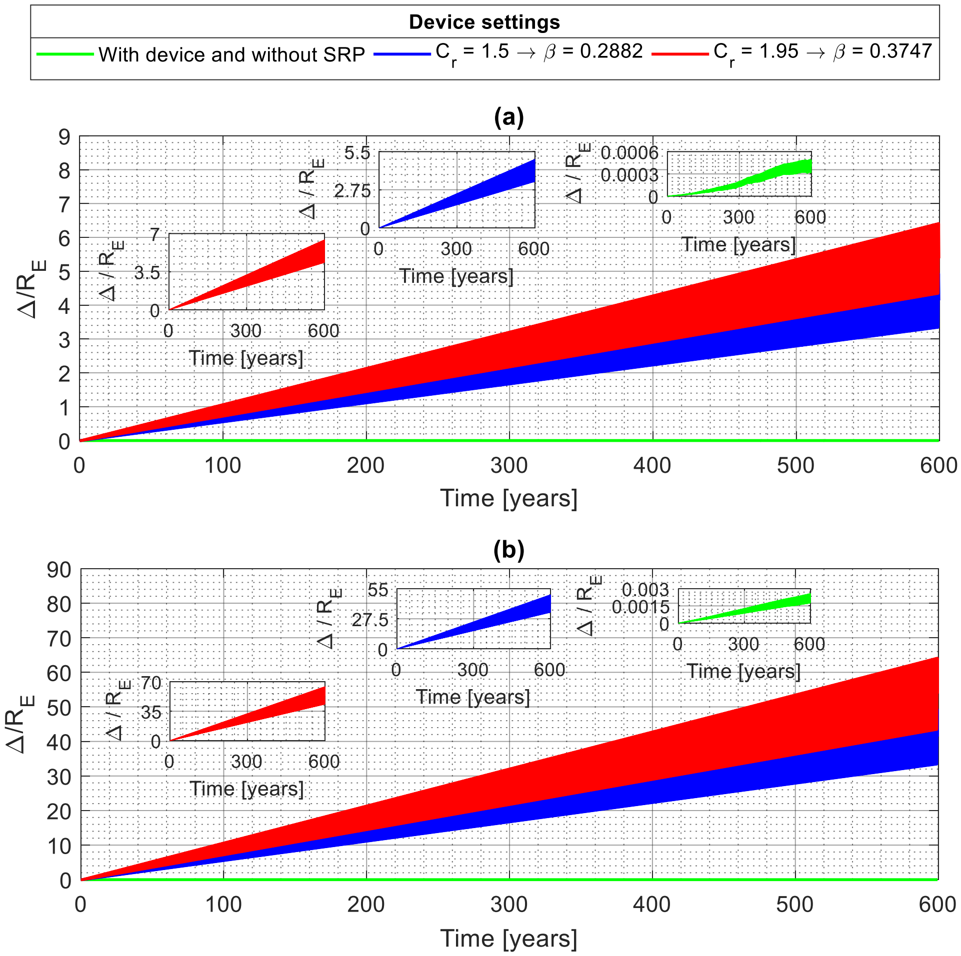

Figure 6. Deviation between the undisturbed and the disturbed orbit in terrestrial radius for Apophis considering ρ = 1 g/m², a tether with 50 km and (a) 2,000 kg and (b) 20,000 kg for the device.

In Figure 7, we have the variation of δ/R_E, the minimum distance asteroid-Earth, for the two asteroids under study, considering a device with 20,000 kg and a tether with 50 km length. The effect of the variation of the tether and the mass of the device in this type of plot is imperceptible and, therefore, the other cases are omitted here. The reason is the domination of the effects of the solar radiation pressure over the displacement of the center of mass of the system, since the mass of the device is small. The maximum distance between each asteroid and Earth occurs when the bodies are positioned at opposite ends of their orbits (at the same instant of time), that is, the asteroid is in the apoapsis and the Earth in the periapsis. The maximum distance reached by Itokawa (approximately 62,500 R_E) is higher than the values reached by Apophis (approximately 50,000 R_E), due to the differences in semi-axis and eccentricity (see Table 1). It is also noted that the frequency of the approximations of Itokawa to Earth is smaller compared to Apophis and Earth. This is due to the fact that the bodies have different orbital periods.

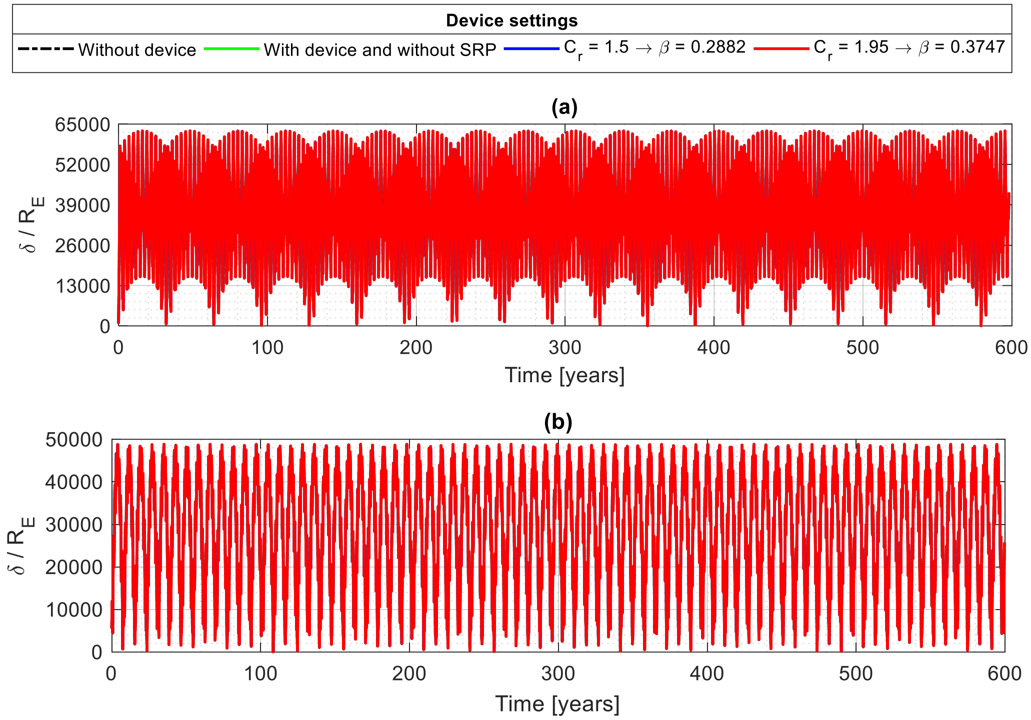

Figure 7. Distance to Earth in terrestrial radius considering ρ = 1 g/m², a 20,000 kg device and 50 km tether for (a) Itokawa (b) Apophis.

In Figure 8 the regions of minimum approximations to Earth (shown in Figure 7) are enlarged to perform the analysis of the effect of the use of the device in the deviations of the trajectory of the asteroid. The green and black curves are practically superimposed, because the displacement caused in the center of mass of the system with the inclusion of the device (without SRP) is very small. The inclusion of the effect of the SRP can help the deviation or approach of the asteroid with the Earth. It gives the possibility of two types of space missions: planetary defense and exploration/mining. The increase of the mass of the device implies in the increase of its geometric dimensions and thus amplifies the deviations, as we see by comparing Figures 8a with 8b (Itokawa), and 8c with 8d (Apophis). In particular, in the last zoom of Figure 8b we found that a high risk approximation of approximately 4.5 R_E could be extended to approximately 25 R_E when using a device made of material whose coefficient of reflectivity is 1.95. In contrast, a device of 2,000 kg could reduce the approach distance of the asteroid with the Earth to about 1.75 R_E after 579.33 years, as shown in Figure 8a. In the case of Apophis, for the initial conditions used in the simulations, the use of the device would help the planetary defense mission of up to 473 years, as shown in Figure 8c and 8d. After this date, the single passage approaching 200 R_E (up to 600 years) would be reduced by approximately 4 R_E for a device with 2,000 kg and 39 R_E for a device with 20,000 kg, both made with material with coefficient of reflectivity of 1.95. In the first zoom of Figure 8d it is visible that it is possible to deflect the Apophis until 9 R_E in a period of 108 years. This deviation is considerable compared to other long-term methods, such as the gravity tractor.

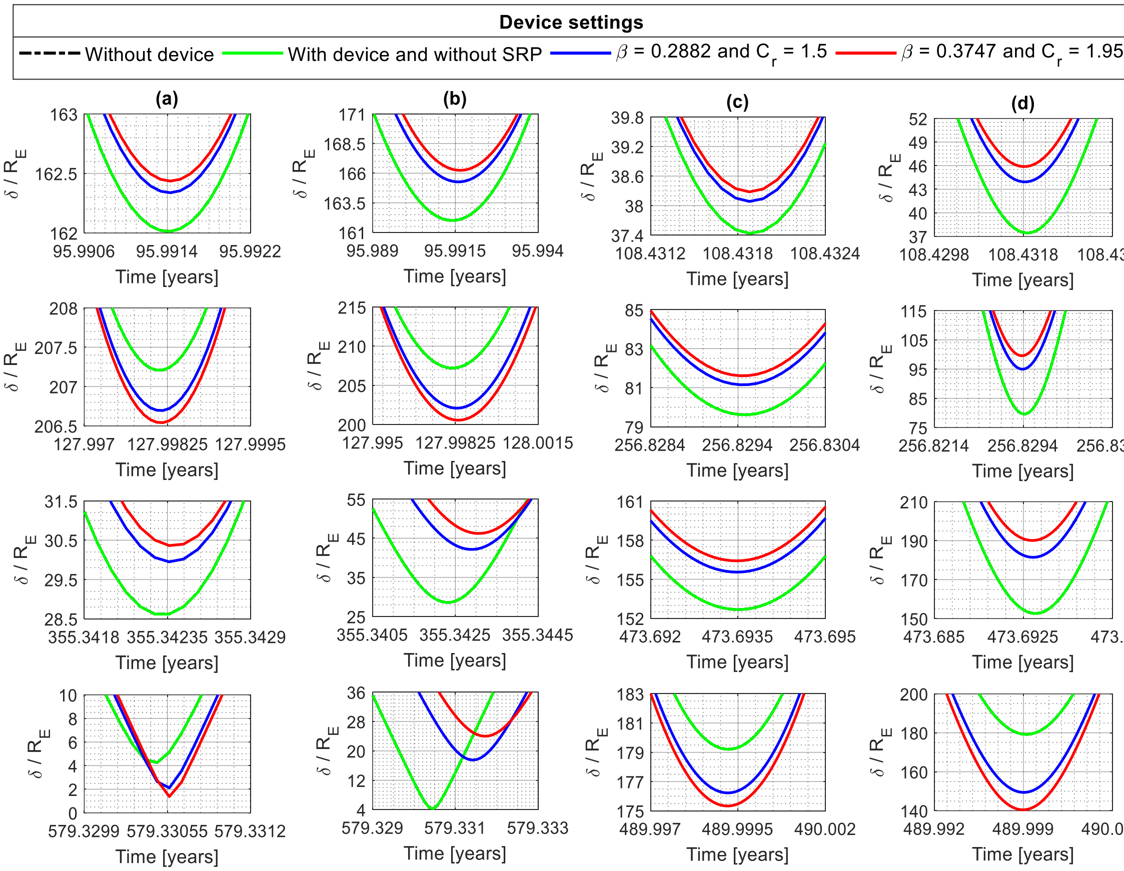

Figure 8. Approximation points between PHA and Earth in terrestrial radius considering ρ = 1 g/m² and tether length of 50 km (a) Itokawa with device of 2,000 kg (b) Itokawa with device of 20,000 kg (c) Apophis with device of 2,000 kg (d) Apophis with device of 20,000 kg.

Next, the same simulations are made using a reflective surface with a density of 0.1 g/m². The goal is to get larger area-to-mass ratios, which increases the effects of the solar radiation pressure. The results show that the effects are much higher. Figure 9 shows the deviation between unperturbed and perturbed orbits for Itokawa considering a 50 km tether and a device mass of 2,000 kg and 20,000 kg. The ratio of the variation amplitudes is now about 1 R_E per 15 years for the device with a mass of 2,000 kg and 1 R_E per 1.5 years for the device with a mass of 20,000 kg. This last value is very large compared with other methods proposed in the literature. Larger deviations can be done with the use of more than one device inserted in the asteroid.

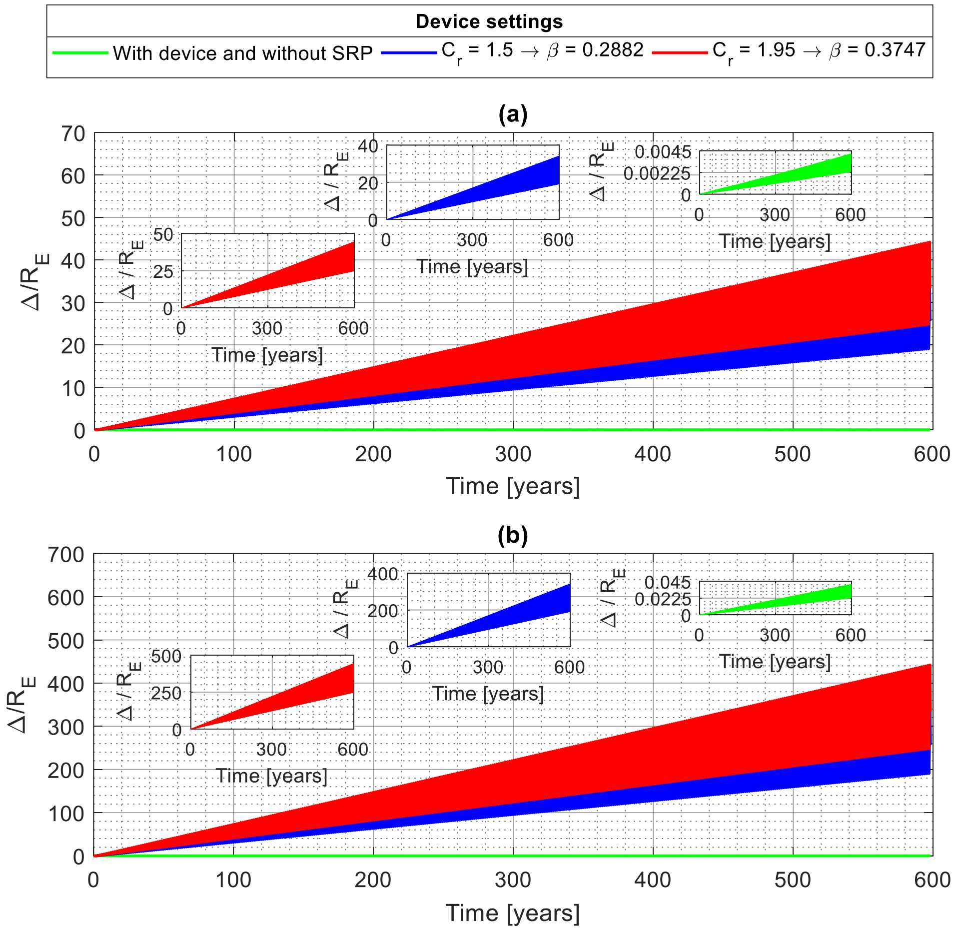

Figure 9. Deviation between undisturbed and perturbed orbits in terrestrial radius for Itokawa considering ρ = 0.1 g/m² and a 50 km tether for a mass of the device of (a) 2,000 kg (b) 20,000 kg.

Figures 10a and 10b show the same deviation between unperturbed and perturbed orbits for Apophis, also considering a 50 km tether and devices with masses of 2,000 kg and 20,000 kg. The ratio of the variation amplitudes is now more than 1 R_E per 10 years for the device with a mass of 2,000 kg and more than 1 R_E per year for the device with a mass of 20,000 kg when $C_r = 1.95$ (red curve). We perform the same type of analysis for $C_r = 1.5$ (blue curves) and the ratio of the variation amplitudes is about 0.82 R_E per 10 years for the device with a mass of 2,000 kg, and about 0.82 R_E per year for the device with a mass of 20,000 kg.

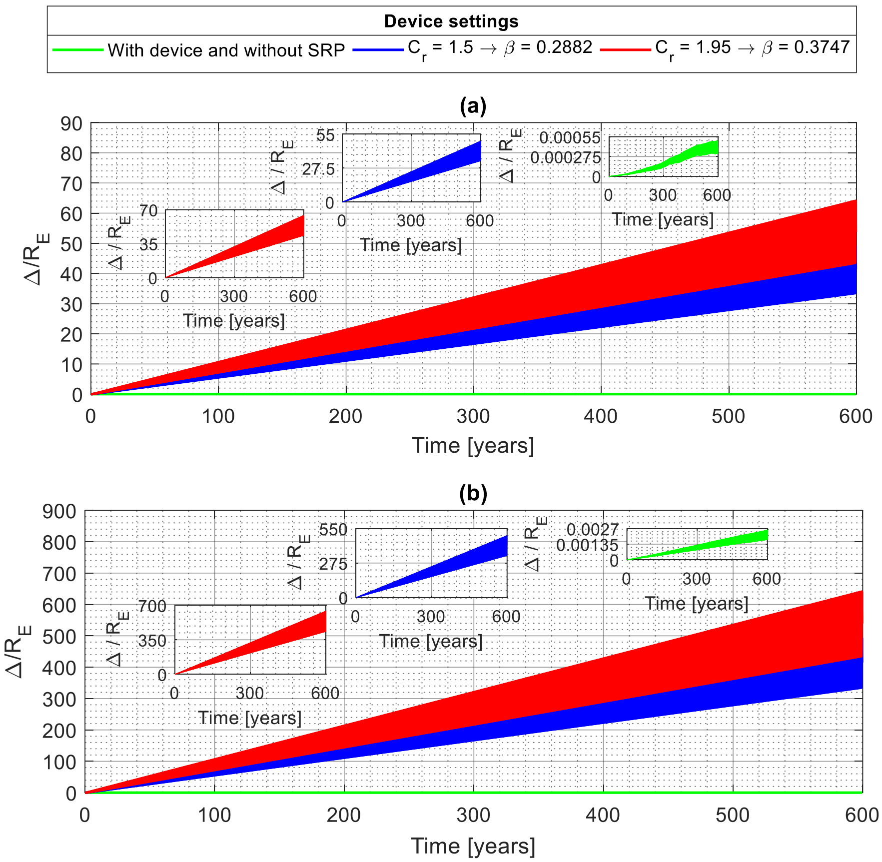

Figure 10. Deviation between undisturbed and perturbed orbits in terrestrial radius for Apophis considering ρ = 0.1 g/m² and a 50 km tether for a mass of the device of(a) 2,000 kg (b) 20,000 kg.

The details of the differences of the models are shown in Figure 11. In general, the use of a light material for the device increases 10 times the deviations observed, which is a quite good result. Approximations below 200 R_E are highlighted (black rectangle) and will be studied separately. Figure 12 shows a zoom of those differences.

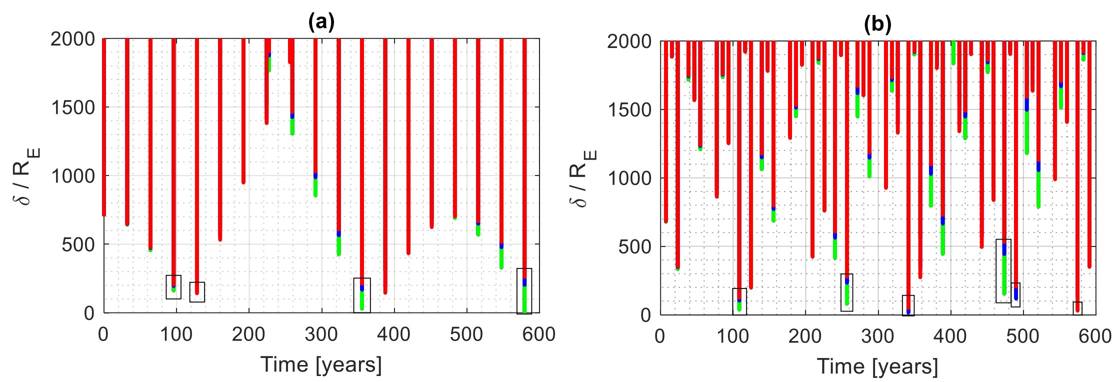

Figure 11. Approximation points between PHA and Earth in terrestrial radius considering ρ = 0.1 g/m², a device with mass of 20,000 kg and tethers with 50 km length for (a) Itokawa (b) Apophis.

In Figures 12a and 12b it is observed that, in 95 years, the asteroid Itokawa can be deflected by 4 R_E (device with 2,000 kg) and 45 R_E (device with 20,000 kg) when considering C_r = 1.95. Moreover, in 579 years a dangerous approximation (4 R_E) could be diverted to 21 R_E (device with 2,000 kg) or 256 R_E (device of 20,000 kg). In the case of Apophis, in 108 years deviations of 9 R_E (device with 2,000 kg) and 93 R_E (20,000 kg device), as shown in Figures 12c and 12d. However, in the last zoom of Figure 12d it is also observed that, in 574 years, Apophis makes a passage at 140 R_E and 25 R_E away from Earth when C_r = 1.5 and C_r = 1.95, respectively. Therefore, the use of solar radiation pressure can be used both to deflect and to bring the PHA closer to Earth.

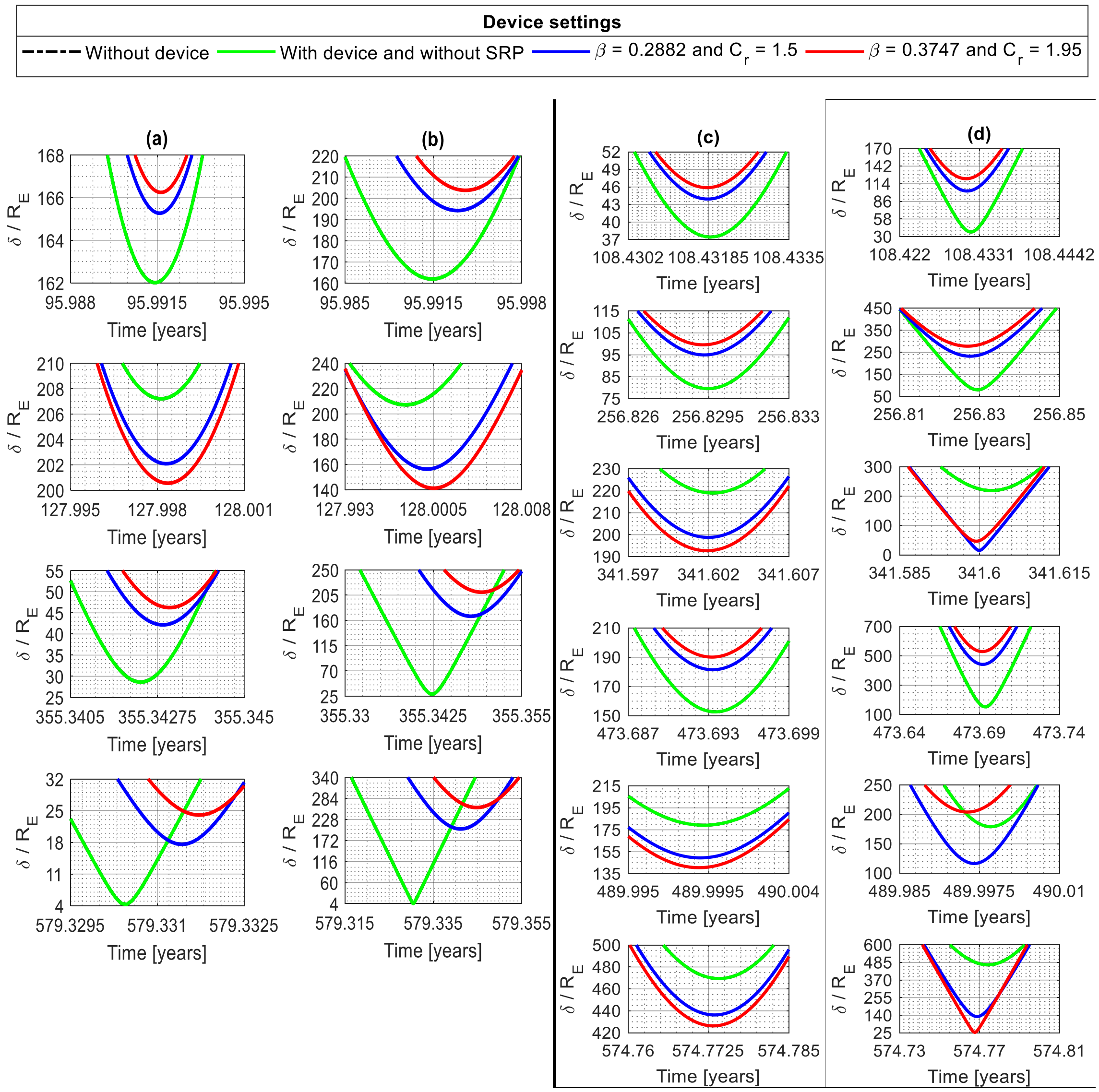

Figure 12. Approximation points between PHA and Earth in terrestrial radius considering ρ = 0.1 g/m² and tether length of 50 km (a) Itokawa with device of 2,000 kg (b) Itokawa with device of 20,000 kg (c) Apophis with device of 2,000 kg (d) Apophis with device of 20,000 kg.

CONCLUSIONS

This paper had the goal of investigating an alternative solution to deflect asteroids that have risks of collision with the Earth. This alternative makes use of one device (or several) with a large area/mass ratio that is attached to the asteroid by a tether to use the solar radiation pressure to deflect the trajectory of the asteroid. The technique suggested deviates the asteroid as a whole, avoiding unpredictable situations due to fragmentation (nuclear explosions or kinetic impact).

In this situation, there are two effects modifying the trajectory of the asteroid, the force coming from the solar radiation pressure, and the displacement of the center of mass of the system due to the presence of the mass of the device inserted in the asteroid. The deviations coming from the solar radiation pressure are much higher and dominates the scenario, because the mass of the device is much smaller than the mass of the asteroid. In 600 years, the highest deviation (Δ) due to the displacement of the center of mass of the system is of the order of 0.5 R_E, considering a tether length of 5,000 km (Itokawa). Furthermore, these deviations are nearly proportional to the mass of the device, and inversely proportional to the mass of the asteroid. Therefore, this technique is very adequate for smaller bodies.

For some orbit geometries, the effects of the solar radiation pressure and the displacement of the center of mass act in the same direction, but sometimes they are in opposite directions. The SRP can make the asteroid to diverge or approach the Earth. It gives the possibility of two types of space missions: planetary defense and exploration, such as mining.

The use of a reflective surface with a density of 0.1 g/m² gives much better results, with larger deviations in the trajectory of the asteroid. It gives a larger area-to-mass ratio, which increases the effects of the solar radiation pressure. This light material for the device increases about 10 times the deviations observed. Lightweight devices are more feasible for tethers with large lengths, but this method is feasible for shorter tethers also, which helps in the engineering construction of the device.

Simulations made for asteroid Apollo (mass of 10^{12} kg) showed values of Δ/R_E much lower than the ones obtained when using Itokawa and Apophis, with mass of the order of 10^{10} kg. This demonstrates that the devices considered in this paper are applicable to less massive asteroids. However, the use of a configuration composed of several devices with even larger dimensions could be used to deflect more massive asteroids than those used in the numerical simulations of this work.

ACKNOWLEDGMENTS

The authors wish to express their appreciation for the support provided by grants# 406841/2016-0, 301338/2016-7, and 140501/2017-7 from the National Council for Scientific and Technological Development (CNPq), and grants# 2014/22295-5, 2016/14665-2, 2016/24561-0, from São Paulo Research Foundation (FAPESP). We also are grateful for the financial support from the National Council for the Improvement of Higher Education (CAPES).

F. C. F. Venditti is supported by NASA's Near-Earth Object Observations Program at the Arecibo Observatory through grants no. NNX12AF24G and NNX13AF46G.

REFERENCES

[1] M.C. Nolan, C. Magri, E.S. Howell, L.A. Benner, J.D. Giorgini, C.W. Hergenrother, R.S. Hudson, D.S. Lauretta, J.L. Margot, S.J. Ostro, and D.J. Scheeres, "Shape model and surface properties of the OSIRIS-REx target Asteroid (101955) Bennu from radar and lightcurve observations." *Icarus*, Vol. 226, No. 1, 2013, pp. 629-640.

[2] A.W. Harris and J.S. Lagerros, "Asteroids in the thermal infrared." *Asteroids III*, University of Arizona, Tucson, 2002, pp. 205-218.

[3] R.S. Hudson. and S.J. Ostro, "Shape and non-principal axis spin state of asteroid 4179 Toutatis." Science, Vol. 270, No. 5233, 1995, pp. 84-86.

[4] C. Colombo, "Optimal Trajectory Design for Interception and Deflection of Near Earth Objects." PhD Thesis, University of Glasgow, 2010.

[5] A.F. Cheng, A.S. Rivkin, P. Michel, J. Atchison, O. Barnouin, L. Benner, N.L. Chabot, C. Ernst, E.G. Fahnestock, M. Kueppers, and P. Pravec, "AIDA DART asteroid deflection test: Planetary defense and science objectives." *Planetary and Space Science*, Vol. 157, 2018, pp. 104-115.

[6] M. Vasile and C.A. Maddock, "On the deflection of asteroids with mirrors." *Celestial Mechanics and Dynamical Astronomy*, Vol. 107, No. 1-2, 2010, pp. 265-284.

[7] W.F. Bottke Jr, D. Vokrouhlický, D.P. Rubincam, and D. Nesvorný, "The Yarkovsky and YORP effects: Implications for asteroid dynamics." *Annual Review of Earth and Planetary Science,* Vol. 34, 2006, pp. 157-191.

[8] Y. Gao and J. Wu, "The optimal control for the tethered system formed by an asteroid and a solar sail." *Advances in Space Research*, Vol. 105, 2009, pp.159-177.

[9] E.T. Lu and S.G. Love, "Gravitational tractor for towing asteroids." *Nature*, Vol. 438, No. 7065, 2005, pp. 177-178.

[10] S. Gong, J. Li, and H. BaoYin, "Formation flying solar-sail gravity tractors in displaced orbit for towing near-Earth asteroids." *Celestial Mechanics and Dynamical Astronomy*, Vol. 57, No 4, 2016, pp.1002-1014.

[11] M.J. Mashayekhi and A.K. Misra, "Tether Assisted Near Earth Object Diversion." *Acta Astronautica*. Vol. 75, 2012, pp. 71–77.

[12] M.J. Mashayekhi and A.K. Misra, "Effect of the Finite Size of an Asteroid on its Deflection Using a Tether-Ballast System." *Celestial Mechanics and Dynamics Astronomy*. Vol. 125, No. 3, 2016, pp. 363-380.

[13] D.B. French and A.P. Mazzoleni, "Asteroid Diversion Using a Long Tether and Ballast." *Journal and Spacecraft and Rockets*. Vol. 46, No. 3, 2009, pp. 645–661.

[14] F.C.F. Venditti and A.K. Misra, "Deflection of a Binary Asteroid System Using Tethers." *Proceedings*…Israel: Jerusalem, 66th International Astronautical Congress, IAC-15-D4.3.1, 2015.

[15] F.C.F. Venditti, L.O. Marchi, A.K. Misra, and A.F.B.A. Prado, "Dynamics of Tethered Binary Asteroid Systems." *Proceedings*…, 49th Lunar and Planetary Science Conference, LPSC #1885, 2018.

[16] V.G. Vil'ke, E.N. Chumachenko, D.W. Dunham, and R.R. Nazarov, "Motions of two tethered asteroids." *Cosmic Research*, Vol. 51, No. 4, 2013, pp. 315-318.

[17] S.S. Cohen and A.K. Misra, "Elastic oscillations of the space elevator ribbon." *Journal of Guidance, Control, and Dynamics*, Vol. 30, No. 6, 2017, pp. 1711-1717.

[18] P. Woo and A.K. Misra, "Mechanics of very long tethered systems." *Proceedings*…Hawaii: Honolulu, Astrodynamics Specialist Conference and Exhibit, AAS/AIAA, 2008.

[19] A.K. Misra, "Dynamics and control of tethered satellite systems." *Acta Astronautica*, Vol. 63, No. 11-12, 2008, pp. 1169-1177.

[20] V. Aslanov and V. Yudintsev, "Dynamics of large space debris removal using tethered space tug." *Acta Astronautica*, Vol. 91, 2013, pp. 149–156.

[21] R. D. Estes, E. C. Lorenzini, J. Sanmart-egrave, n, J. Pel-Uuml, ez, M. Mart-egrave, nez-S-UUml, nchez, C.L. Johnson, and I.E. Vas., "Bare tethers for electrodynamic spacecraft propulsion." *Journal of Spacecraft and Rockets*, Vol. 37, No. 2, 2000, pp. 205–211.

[22] M.K. Ammar, "The Effect of Solar Radiation Pressure on the Lagrangian Points in the Elliptic Restricted Three-Body Problem." *Astrophysics and Space Science*. Vol. 313, No. 4, pp. 393–408, 2008.

[23] D. Vokrouhlicky, W.F. Bottke, S. R. Chesley, D.J. Scheeres, and T.S. Statler, "The Yarkovsky and YORP effects." *Space Science Series Book: Asteroids IV,* DOI: 10.2458/azu_uapress_9780816532131-ch027, 2015, pp. 509-531.

[24] D. Farnocchia, S.R. Chesley, P.W. Chodas, M. Micheli, D. J. Tholen, A. Milani, G. T. Elliott, and F. Bernardi, "Yarkovsky-driven impact risk analysis for asteroid (99942) Apophis." *Icarus*, Vol. 224, No. 1, 2013, pp. 192–200.

[25] B. Dachwald and B. Wie, "Solar sail kinetic energy impactor trajectory optimization for an asteroid-deflection mission." *Journal of Spacecraft and Rockets*, Vol. 44, No. 4, 2007, pp. 755–764.

[26] S. Kikuchi and J. Kawaguchi, "Asteroid de-spin and deflection strategy using a solar-sail spacecraft with reflectivity control devices." *Acta Astronautica*. DOI: https://doi.org/10.1016/j.actaastro.2018.06.047, 2018.

[27] K. Berry, B. Sutter, A. May, K. Williams, B.W. Barbee, M. Beckman, and B. Williams, "OSIRIS-REx touch-and-go (TAG) mission design and analysis.", *Proceedings*…Colorado: Breckenridge, 36th Annual AAS Guidance Control Conference, AAS/AIAA, 2013.

[28] D.S. Lauretta, S.S. Balram-Knutson, E. Beshore, W.V. Boynton, C.D. d'Aubigny, D.N. DellaGiustina, H.L. Enos, D.R. Gholish, C.W. Hergenrother, E.S. Howell, C.A. Johnson, E.T. Morton, M.C. Nolan, B. Rizk, H.L. Roper, A.E. Bartels, B.J. Bos, J.P. Dworkin, D.E. Highsmith, D.A. Lorenz, L.F. Lim, R. Mink, M.C. Morean, J.A. Nuth, D.C. Reuter, A.A. Simon, E.B. Bierhaus, B.H. Bryan, R. Ballouz, O.S. Barnouin, R.P. Binzel, W.F. Bottke, V.E. Hamilton, K.J. Walsh, S.R. Chesley, P.R. Christensen, B.E. Clark, H.C. Connolly, M.K. Crombie, M.G. Daly, J.P. Emery, T.J. McCoy, J.W. McMahon, D. J. Scheeres, S. Messenger, K. Nakamura, K. Righter, and S.A. Sandford, "OSIRIS-REx: sample return from asteroid (101955) Bennu." *Space Science Reviews*, Vol. 212, No. 1-2, 2017, pp. 925–984.

[29] O. Montenbruck and E. Gill, *Satellite Orbits: Models, Methods and Applications*. Springer, 2005.

[30] C.R. McInnes, "*Solar sailing: technology, dynamics and mission applications*." Germany: Springer, 1 ed., 1999.

[31] C. Garner, B. Diedrich and M. Leipold, "*A summary of solar sail technology developments and proposed demonstration missions."* NASA Technical Reports. JPC-99-2697, Pasadena, California, United States, 1999.

[32] V. Badescu, R.B. Cathcart and R.D. Schuiling, *Macro-engineering: a challenge for the future*. Netherlands: Springer, 1 e.d., 2006.